

ELECTRICAL BEHAVIOUR RELATED TO STRUCTURE OF NANOSTRUCTURED GeSi FILMS ANNEALED AT 700°C

Ana-Maria Lepadatu^{1,2}, Ionel Stavarache¹, Adrian Maraloiu¹, Catalin Palade¹, Teodorescu Valentin Serban¹, Ciurea Lidia Magdalena^{1,3}

¹National Institute of Materials Physics, Magurele 077125, Romania

²University of Bucharest, Faculty of Physics, Magurele 077125, Romania

³Academy of Romanian Scientists, Bucuresti 050094, Romania

Email: lepadatu@infim.ro, stavarache@infim.ro, maraloiu@infim.ro, catalin.palade@infim.ro, teoval@infim.ro, ciurea@infim.ro

Abstract—In this paper we continue the previous investigations on nanostructured Ge_xSi_{1-x} films. The films were deposited by magnetron sputtering and annealed in N_2 atmosphere at 700 °C. Their structure was investigated and correlated with the electrical behavior. For this, conventional and high-resolution transmission electron microscopy together with selected area electron diffraction was used. Electrical measurements of current-voltage and current-temperature curves were made. The majority of crystallites that forms the films have the composition $Ge_{50}Si_{50}$ and 15 – 30 nm size. The $I - T$ characteristics have Arrhenius dependence, with two activation energies interpreted as transitions between quantum confinement levels.

Keywords: SiGe nanocrystals; Magnetron sputtering; TEM; electrical properties.

1. INTRODUCTION

GeSi nanocrystals (GeSi ncs) have received much attention in recent years, due to their interesting electrical and optoelectronic properties, which are very promising for improving of nano-based devices [1–5]. Thus, GeSi ncs present strong quantum confinement (QC) effect, compared with Si ncs and have the advantage of the fine tuning of energy band structure [6, 7], by alloying. These properties recommend them for optoelectronic devices which work from mid to far infrared range [8, 9].

The films containing GeSi ncs embedded or not in amorphous SiO_2 matrix are usually (co-) deposited by the magnetron sputtering method followed by the thermal annealing [4, 10, 11].

In this work, we draw our attention on preparation, structure and electrical investigations of GeSi nanostructures. The preparation of films is described and the results obtained from structure investigations and electrical characterization (current-voltage, $I - V$ and current-temperature, $I - T$ measurements) are

presented and discussed.

2. EXPERIMENTAL

Amorphous Ge_xSi_{1-x} layers were prepared using a magnetron sputtering deposition equipment with a confocal geometry [12]. The Si and quartz substrates were wet cleaned, keeping the native SiO_2 layer of about 4 nm thickness on Si wafers. The deposition chamber was evacuated to $<10^{-7}$ Torr and then, Ar (5N) was introduced into the chamber. The deposition was performed in DC regime using two targets of Si and Ge respectively, for a chosen Ge:Si composition of 55:45. The Ar flow was maintained at 20 sccm, ensuring a 4 mTorr work pressure. The deposition was followed by annealing in purged N_2 , in a conventional atmospheric oven at 700°C. For electrical measurements, Al electrodes were thermally deposited in a coplanar geometry.

To further observe the microstructure of the GeSi films the conventional transmission electron microscopy (TEM) and high-resolution TEM (HRTEM) together with selected area electron diffraction (SAED) were used. The specimens for TEM were prepared by the conventional cross section method. TEM and SAED images were collected using the JEM ARM 200F high resolution electron microscope. The structure investigations were made on films with Si substrate (native oxidized), allowing the SAED with Si lattice reference. The films microstructure is the same for both quartz and Si substrates.

Electrical measurements ($I - V$ and $I - T$) were performed on annealed samples deposited on quartz. The electrical measurements were performed in a cryostat (10 – 500 K), using a 6517A electrometer and a temperature controller, and controlled by a program developed in

LabVIEW 8.5.1 environment.

3. RESULTS AND DISCUSSIONS

Figure 1 shows the low magnification images of the GeSi layer deposited on Si substrate in two situations: as deposited and after annealing at 700 °C. As one can see, the initial structure of the film is amorphous and after annealing it is crystalline. At the same time, the film thickness diminishes from 185 nm before annealing to 160 nm after it. The as grown film has a porosity in-between the columnar morphology and it is visible as white traces perpendicular to the film surface.

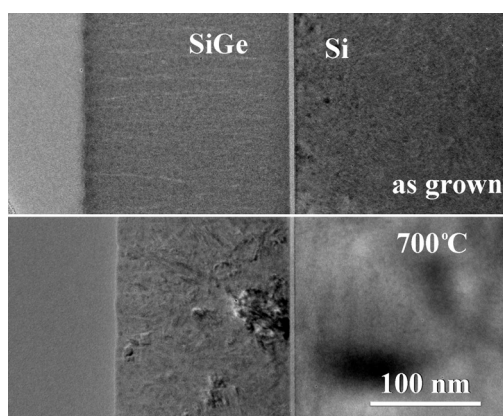


Fig. 1. Low magnification images of the as grown film and annealed one at 700°C.

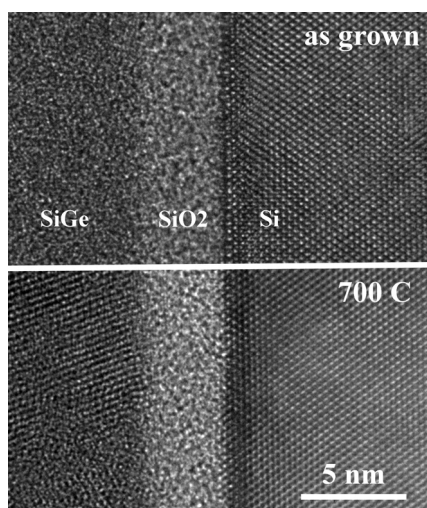


Fig. 2. HRTEM images of the film/substrate interface before and after annealing.

Figure 2 presents the native SiO₂ layer on Si substrate at the interface with the GeSi film, with 3.5 nm thickness unchanged after the annealing process.

The precise films thickness determinations were performed after orientation of the specimen

in the microscope with Si substrate in <110> zone axis. This orientation corresponds with the exact alignment of the electron beam axis with the surface of the GeSi film. This alignment can be observed in high resolution images in Fig. 2 and in SAED pattern in Fig. 3.

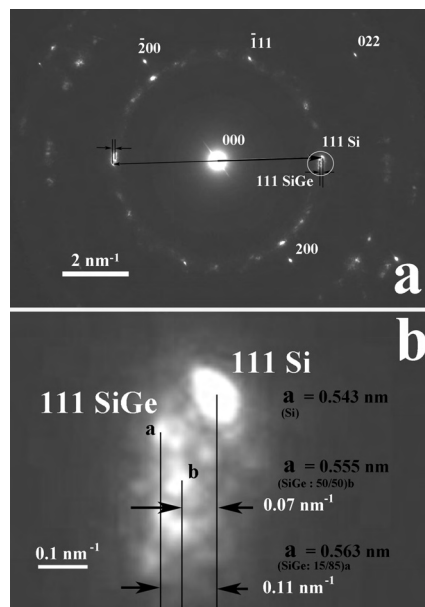


Fig. 3. SAED diffraction pattern from an area selected near the Si interface, which shows diffraction spots from the GeSi film and the Si substrate: **a)** the Si substrate is in <110> orientation, and the spot 111 of Si is well aligned with a group of spots coming from the GeSi ncs; **b)** a 15 time magnification image of the 111 group of spots from **a)**.

The SAED was collected from an area with 150 nm diameter which also contains some part of the substrate. This pattern (Fig. 3) shows spots from the <110> zone axis of the Si substrate and reflections coming from the GeSi crystallites in the GeSi film. The area selected for the SAED pattern and the position of this area were chosen to obtain a diffraction pattern where the intensity of the reflection spots coming from the film and the substrate are quite equal. This gives the possibility to measure the lattice constant of the GeSi crystallites having the Si lattice parameter as reference. This is exposed in the detail of the diffraction spots in Fig. 3b. This analysis shows the presence of a dispersion of lattice constant, corresponding to a variation of the Ge content in the GeSi lattice.

The majority of the spots coming from the GeSi crystallites (in the area b, GeSi spots located at a distance of 0.07 nm⁻¹) show a lattice parameter of 0.555 nm, which correspond to the GeSi 50/50 composition. However, some of the crystallites indicate a larger lattice parameter of

about 0.563 nm, which correspond to the GeSi 85/15 composition (in the area a, some spots are located at distance of about 0.11 nm^{-1}). This shows that the initial composition of GeSi (55/45) assured by the magnetron sputtering is distributed in a large number of stoichiometric GeSi 50/50 crystallites and others (much less) which have a higher concentration of Ge.

After annealing, the film crystallizes and its thickness decreases, in respect to the thickness of the as deposited film, by elimination of the inside porosity (XTEM images in Fig. 1). This initial porosity appears in-between the columnar growth morphology which is very common for sputtered films. The annealed films have no porosity at the boundaries between the crystallites (Fig. 1) and the sizes of crystallites are in the 15 – 30 nm range.

The $I - V$ characteristic taken at room temperature on annealed film is presented in Fig. 4. As one can see, the curve is symmetrical in bias polarization, linear at low voltages (around 0 V) and superlinear up to 5V.

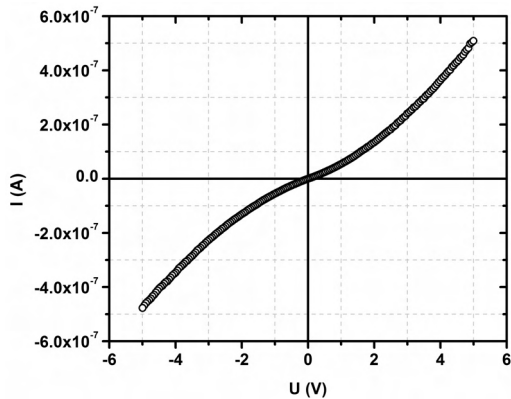


Fig. 4. $I - V$ characteristic measured at room temperature, on annealed film.

The $I - T$ characteristics measured in the 80 – 300 K temperature interval, for different bias polarizations (1, 3 and 5 V) are given in Fig. 5. These curves have an Arrhenius dependence on temperature and present two activation energies at low and high temperatures, namely $E_{a1} = 0.15 \text{ eV}$ and $E_{a2} = 0.23 \text{ eV}$, respectively.

Taking into consideration the results obtained from microstructure measurements, i.e. the GeSi films are formed mainly of GeSi ncs with rather high diameters (15 – 30 nm), we can apply our QC model [13, 14, 15, 176] in order to identify the QC levels on which the electron transitions take place.

We have to remark that the QC model is a very good approximation in the case of small

nanocrystals (quantum dots), but we can use it in order to estimate the average diameter. In our films, the crystallites are large enough to have an energy band structure formed by quasibands (and not by discrete QC levels).

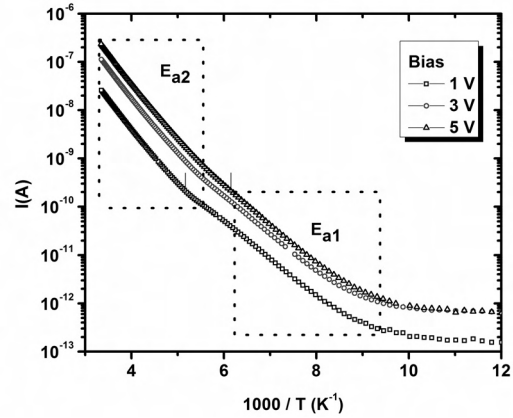


Fig. 5. $I - T$ curves taken on films annealed at 700°C .

By considering as initial data E_{a1} and E_{a2} obtained from experiments, we determined the average diameter of crystallites and compared it with the value obtained from the microstructure measurements. We used the effective mass of the stoichiometric composition of GeSi bulk semiconductor, $m^* = 0.26 m_0$, where m_0 is the free electron mass. The electron transitions take place between levels $|n, l\rangle$ and $|n', l'\rangle$, so that $\Delta l = 0$. Thus, the transition corresponding to E_{a1} is between $|1, 2\rangle$ and $|2, 2\rangle$, and corresponding to E_{a2} is between $|2, 2\rangle$ and $|3, 2\rangle$. The determined average diameter is 15 nm, instead of 20 nm (experimental value). This rather high difference between the calculated and the experimental diameters appears because the QC model is applicable to small nanocrystals. Therefore, we can conclude that electron transitions take place between the energy quasibands (or at least between energy levels with width higher than kT).

Transport mechanisms depend on film morphology by the crystallinity, nanocrystals sizes and their distribution in the film [17–19]. In this frame, the superlinear $I - V$ characteristic can be explained by a percolation process taking place in the percolative system of GeSi formed by nanocrystals [20].

4. CONCLUSIONS

In this paper we investigate the structure and electrical behaviour of GeSi films deposited by magnetron sputtering on both Si and quartz substrates, followed by thermal annealing at 700°C . The as deposited films are amorphous and

porous. By annealing, the films crystallize and their thickness diminishes from 185 nm to 160 nm. Also, the thickness of the native SiO₂ layer existing on the surface of the Si wafers remains unchanged after annealing. The SAED and HRTEM investigations reveal that the GeSi films are formed by a majority of Ge₅₀Si₅₀ ncs with sizes in the 15 – 30 nm interval, but crystallites with high Ge content, i.e. Ge₈₅Si₁₅, were evidenced, too.

The $I - T$ characteristics present two activation energies at low and high temperatures, namely $E_{a1} = 0.15$ eV and $E_{a2} = 0.23$ eV, respectively. We applied our QC model and identify the activation energies as transitions between QC levels. Thus, to E_{a1} and E_{a2} correspond the transitions between $|1,2\rangle$ and $|2,2\rangle$, and between $|2,2\rangle$ and $|3,2\rangle$, respectively. $I - V$ characteristics are explained by a percolation process taking place in the GeSi films formed by nanocrystals.

Acknowledgement—This work was supported by the Romanian National Authority for Scientific Research through the CNCS–UEFISCDI Contract PD/0094 33/2011 and Contract IDEI 289/2011.

References

- [1] W.T. Xu, H.L. Tu, D.L. Liu, R. Teng, Q.H. Xiao, Q. Chang, “Self-assembled SiGe quantum dots embedded in Ge matrix by Si ion implantation and subsequent annealing”, *J. Nanopart. Res.*, **14**(1), pp. 682, 2012.
- [2] N. Hrauda, J. Zhang, E. Wintersberger, T. Etzelstorfer, B. Mandl, J. Stangl, D. Carbone, V. Holy, V. Jovanovic, C. Biasotto, L.K. Nanver, J. Moers, D. Grutzmacher, G. Bauer, “X-ray nanodiffraction on a single SiGe quantum dot inside a functioning field-effect transistor”, *Nano Lett.*, **11**(7), pp. 2875–2880, 2011.
- [3] E. Tevaarwerk, P. Rugheimer, O.M. Castellini, D.G. Keppel, S.T. Utley, D.E. Savage, M.G. Lagally, M.A. Erikssona, “Electrically isolated SiGe quantum dots”, *Appl. Phys. Lett.*, **80**(24), pp. 4626–4628, 2002.
- [4] M. Buljan, S.R.C. Pinto, R.J. Kashtiban, A.G. Rolo, A. Chahboun, U. Bangert, S. Levichev, V. Holý, M.J.M. Gomes, “Size and spatial homogeneity of SiGe quantum dots in amorphous silica matrix”, *J. Appl. Phys.*, **106**(8), pp. 084319, 2009.
- [5] D. Mihalache, “Recent trends in micro- and nanophotonics: A personal selection”, *J. Optoelectron. Adv. Mater.*, **13**(9-10), pp. 1055–1066, 2011.
- [6] C.B. Simmons, M. Thalukulam, B.M. Rosemeyer, B.J. Van Bael, E.K. Sackmann, D.E. Savage, M.G. Lagally, R. Joynt, M. Friesen, S.N. Coppersmith, M.A. Eriksson, “Charge sensing and controllable tunnel coupling in a Si/SiGe double quantum dots”, *Nano Lett.*, **9**(9), pp. 3234–3238, 2009.
- [7] Y.M. Yang, X.L. Wu, G.G. Siu, G.S. Huang, J.C. Shen, D.S. Hu, “Formation, structure, and phonon confinement effect of nanocrystalline Si_{1-x}Ge_x in SiO₂-Si-Ge cosputtered films”, *J. Appl. Phys.*, **96**(9), pp. 5239–5242, 2004.
- [8] P. Iamraksa, N.S. Lloyd, D.M. Bagnall, “Si/SiGe near-infrared photodetectors grown using low pressure chemical vapour deposition”, *J. Mater. Sci. Mater. Electron.*, **19**(2), pp. 179–182, 2008.
- [9] P.H. Sun, S.T. Chang, Y.C. Chen, H. Lin, “A SiGe/Si multiple quantum well avalanche photodetector”, *Solid State Electron.*, **54**(10), pp. 1216–1220, 2010.
- [10] E.V. Jelenkovic, K.Y. Tong, W.Y. Cheung, S.P. Wong, B.R. Shi, G.K.H. Pang, “SiGe-Si junctions with boron-doped SiGe films deposited by co-sputtering”, *Solid-State Electron.*, **50**(2), pp. 199–204, 2006.
- [11] S.R.C. Pinto, R.J. Kashtiban, A.G. Rolo, M. Buljan, A. Chahboun, U. Bangert, N.P. Barradas, E. Alves, M.J.M. Gomes, “Structural study of Si_{1-x}Ge_x nanocrystals embedded in SiO₂ films”, *Thin Solid Films*, **518**(9), p. 2569, 2010.
- [12] I. Stavarache, A.M. Lepadatu, I. Pasuk, V.S. Teodorescu, M.L. Ciurea, “Preparation and electrical characterization of SiGe nanostructures”, *CAS 2011, Proc. IEEE CN CFP11CAS-PRT*, **1**, pp. 49–52, 2011.
- [13] V. Iancu, M.R. Mitroi, A.M. Lepadatu, I. Stavarache, M.L. Ciurea, “Calculation of the quantum efficiency for the absorption on confinement levels in quantum dots”, *J. Nanopart. Res.*, **13**(4), pp. 1605–1612, 2011.
- [14] M.L. Ciurea, “Quantum confinement in nanocrystalline silicon”, *J. Optoelectron. Adv. Mater.*, **7**(5), pp. 2341–2346, 2005.
- [15] M.L. Ciurea, V. Iancu, I. Stavarache, “Quantum confinement modeling of electrical and optical processes in nanocrystalline silicon”, *J. Optoelectron. Adv. Mater.*, **8**(6), pp. 2156–2160, 2006.
- [16] A.M. Lepadatu, I. Stavarache, M.L. Ciurea, V. Iancu, “The influence of shape and potential barrier on confinement energy levels in quantum dots”, *J. Appl. Phys.*, **107**(3), pp. 033721, 2010.
- [17] V. Iancu, M. Draghici, L. Jdira, M.L. Ciurea, “Conduction mechanisms in silicon-based nanocomposites”, *J. Optoelectron. Adv. Mater.*, **6**(1), pp. 53–56, 2004.
- [18] A.M. Lepadatu, I. Stavarache, T.F. Stoica, M.L. Ciurea, “Study of Ge nanoparticles embedded in an amorphous SiO₂ matrix with photoconductive properties”, *Digest J. Nanomater. Bios.*, **6**(1), pp. 66–73, 2011.
- [19] I. Stavarache, A.M. Lepadatu, A.V. Maraloiu, V.S. Teodorescu, M.L. Ciurea, “Structure and electrical transport in films of Ge nanoparticles embedded in SiO₂ matrix”, *J. Nanopart. Res.*, **14**, pp. 930, 2012.
- [20] A.K. Sen, “Nonlinear response, semi-classical percolation and breakdown in the RRTN model”, *Quantum and semiclassical percolation and breakdown in disordered solids*, Springer, Berlin Heidelberg, 2009.